Computed Tomography (CT)

Part 1

André Sopczak

Institute of Experimental and Applied Physics,
Czech Technical University in Prague
http://cern.ch/sopczak
andre.sopczak@cvut.cz
based on lectures 2005-2022 by Jan Kybic,
Department of Cybernetics, FEE CTU

2023

Radiation | Types of Ionizing Radiation

Ionizing radiation | Radiation that causes ionization

Particle beams

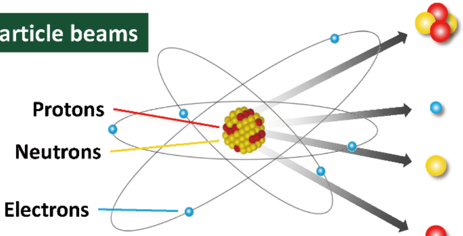

- **α-particles** (helium nuclei ejected from a nucleus)
- **β-particles** (electrons ejected from a nucleus)
- **Neutron beams** (produced in nuclear reactors, accelerators, etc.)
- **Proton beams** (produced in accelerators, etc.)

Electromagnetic waves

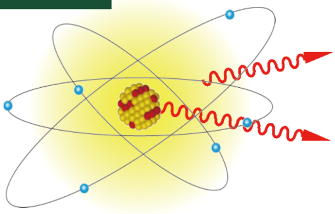

- **X-rays** (generated outside a nucleus)
- **γ-rays** (emitted from a nucleus)

Electromagnetic radiation

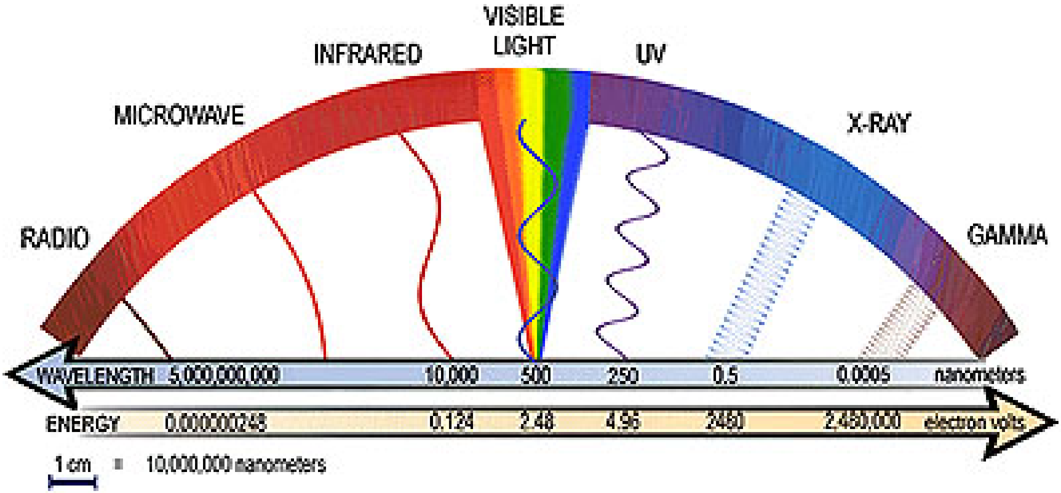

X-rays for CT

- Electro-magnetic waves: no charge, no rest mass
- Corresponding frequency range $10^{15} - 10^{18}$ Hz
- Energies used in medical imaging are in the "hard X-ray" range
- Large penetration depth in light matrices (e.g. tissue)

X-rays interaction with matter

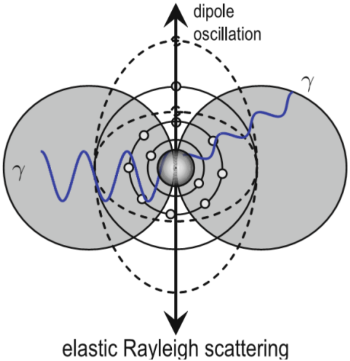

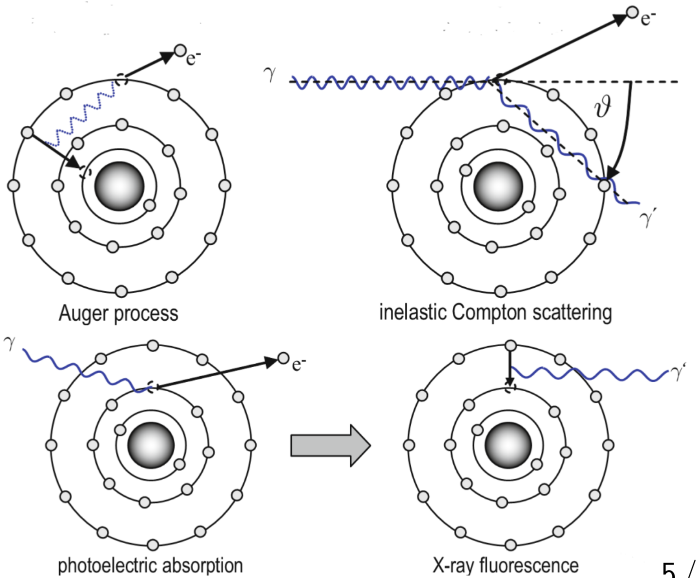

The most relevant processes for attenuation in medical X-ray imaging are:

- Compton scattering
- Photoelectric effect

Computed Tomography (CT) scanner

CT history

1917 mathematical theory (Radon)

1956 tomography reconstruction in radioastronomy (Bracewell)

1963 CT reconstruction theory (Cormack)

1971 CT principles demonstrated (Hounsfield)

1972 first working CT for humans (EMI, London, Hounsfield)

1973 PET, Positron Emission Tomography

1974 Ultrasound tomography

1975 whole body scanner (Hounsfield)

1982 Single Photon Emission Computed Tomography (SPECT)

1985 Helical CT

1998 Multislice CT, 0.5 s/frame

Johann Radon

1887–1956

- born in Děčín (Czech Republic), lived in Göttingen, Brno, Hamburg, Greifswald, Erlangen, Breslau, Innsbruck and Vienna
- mathematician; Radon transform (1917) — reconstruction of a function from its integrals on certain manifolds (projections)

Godfrey Hounsfield

1919–2004

- physicist and engineer (did not attend university)
- worked on radar and on first transistor computers
- created the first CT X-ray scanner
- Nobel prize in Medicine (1979, together with Cormack)

Allan MacLeod Cormack

1924–1998

- born in South Africa, studied in Cambridge, lived in the US
- particle physicist
- theoretical foundation of CT scanning (independently of Hounsfield)
- Nobel prize in Medicine (1979, together with Hounsfield)

CT principles

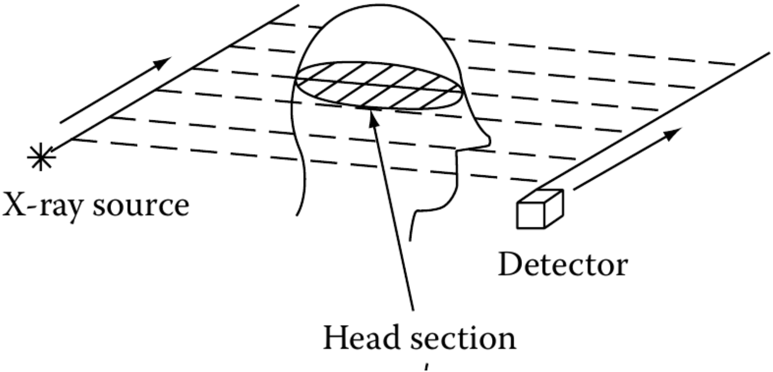

1. Sequence of parallel sections *(tomos)*

CT principles

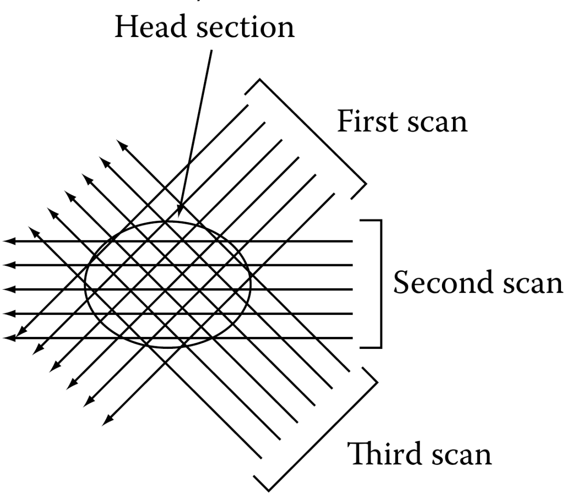

1. Sequence of parallel sections *(tomos)*
2. Sequence of projections from multiple directions

CT principles

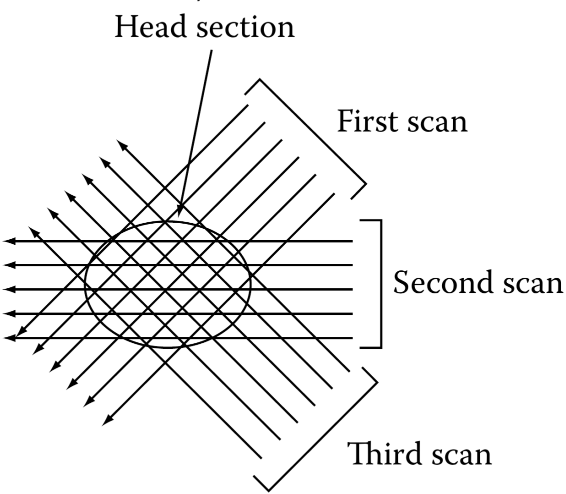

1. Sequence of parallel sections *(tomos)*
2. Sequence of projections from multiple directions
3. Reconstruction of the object

CT example scans

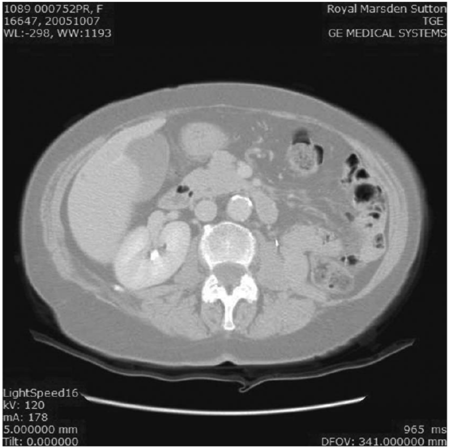

Head and kidneys

CT example scans

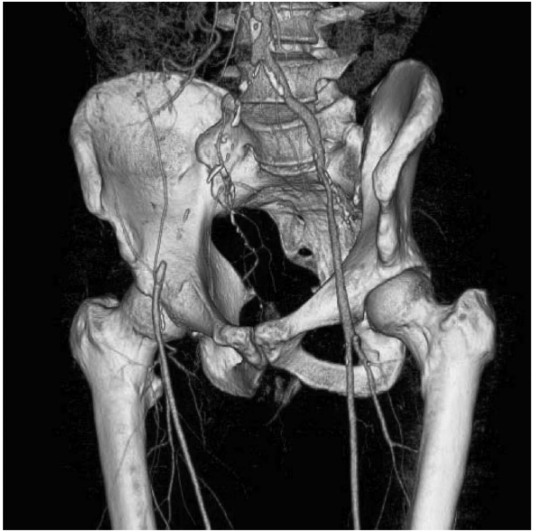

CT angiography, pelvis

Clinical applications

- Lungs

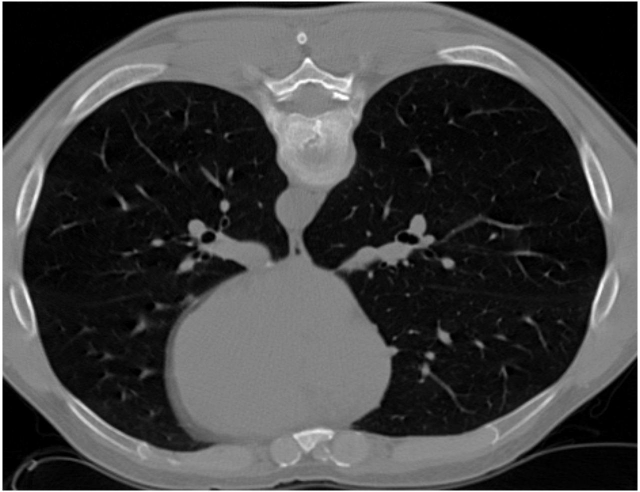

Clinical applications

- Lungs

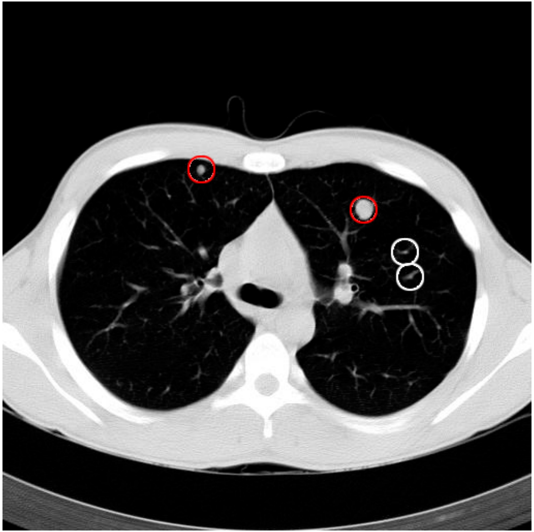

Clinical applications

- Lungs
- Head

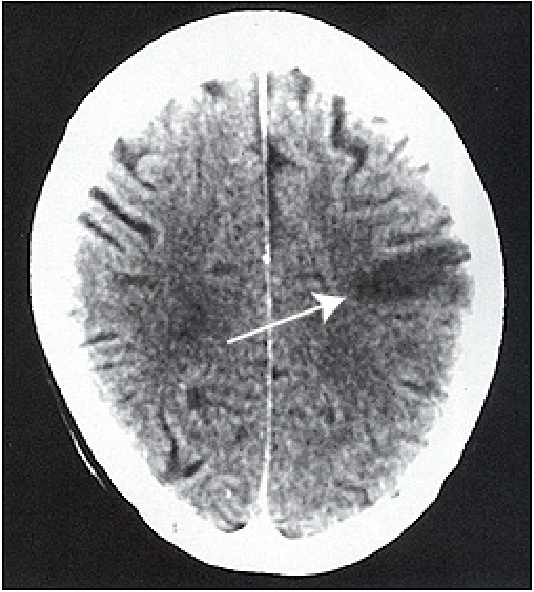

Clinical applications

- Lungs
- Head

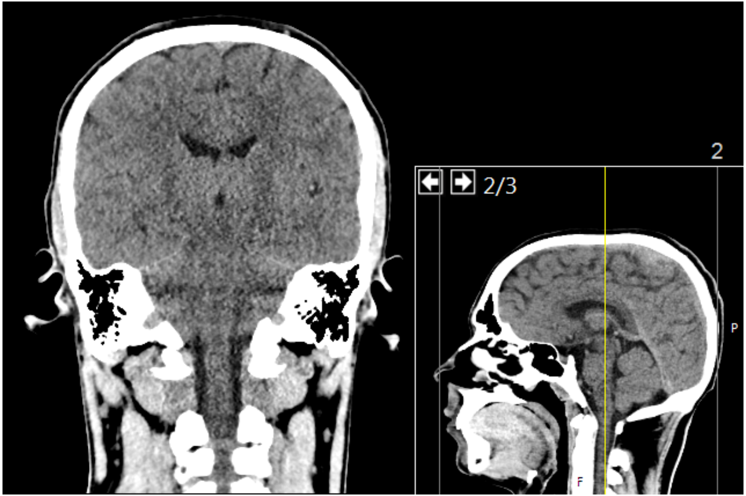

Clinical applications

- Lungs
- Head

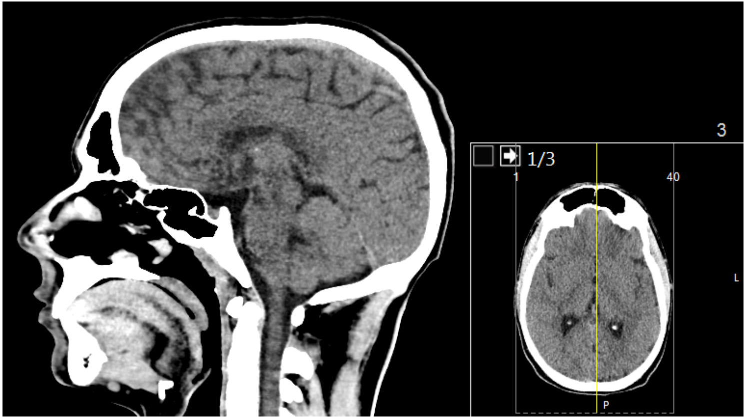

Clinical applications

- Lungs
- Head
- Abdomen

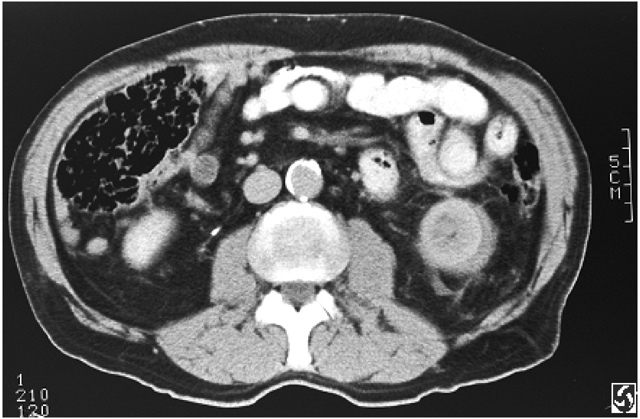

Tomography modalities

- X-rays — CT
- gamma rays — PET, positron emission tomography
- gamma rays — SPECT, single-photon emission computerized tomography
- light — optical tomography
- RF waves — MRI, magnetic resonance imaging
- DC — electric impedance tomography
- ultrasound — ultrasound tomography

First scanner

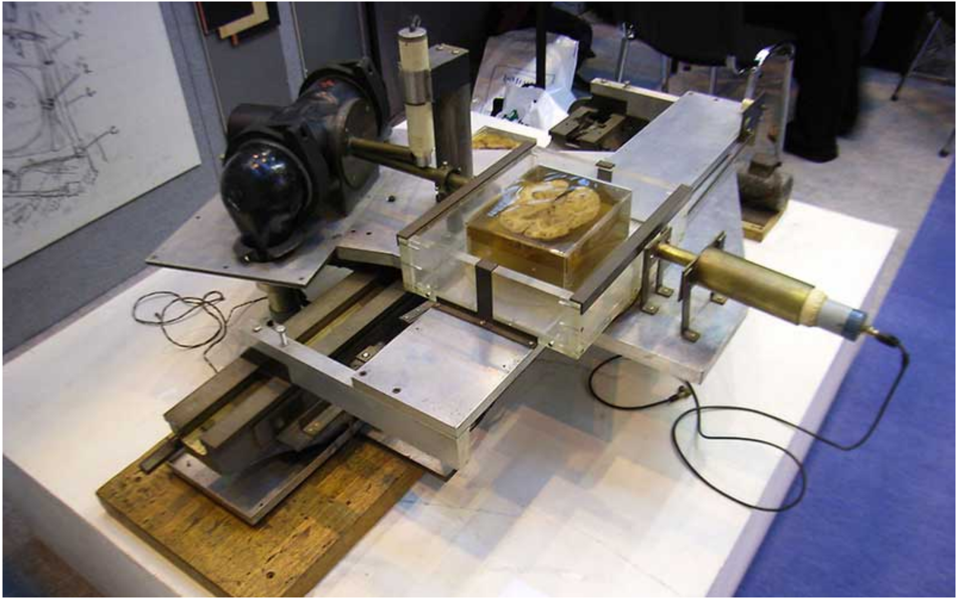

Scanner geometry — generation 1

1971

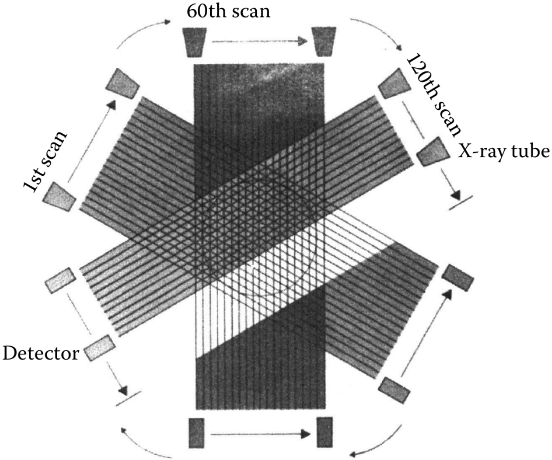

- Single source and single detector
- Finely collimated narrow beam
- Alternating translation and rotation
- Very slow (4 min / section), low resolution
- Low cost, good scatter rejection, easy calibration

Scanner geometry — generation 2

1974

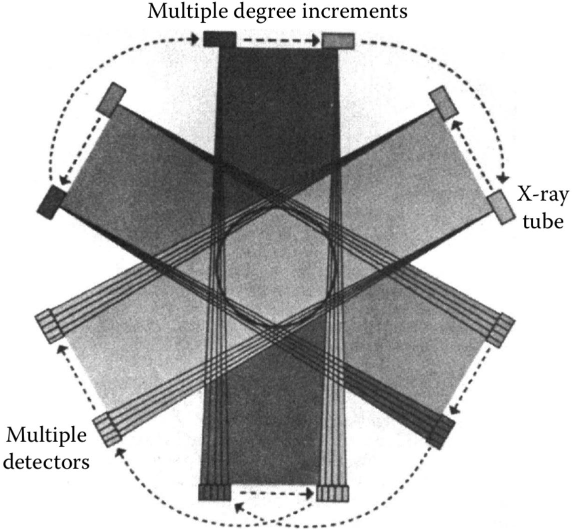

- Narrow fan beam ($\sim 10^\circ$), multiple detectors (N)
- N projections acquired in parallel
- Increased rotation increment
- Increased speed (20 s / section)

Scanner geometry — generation 3

1975

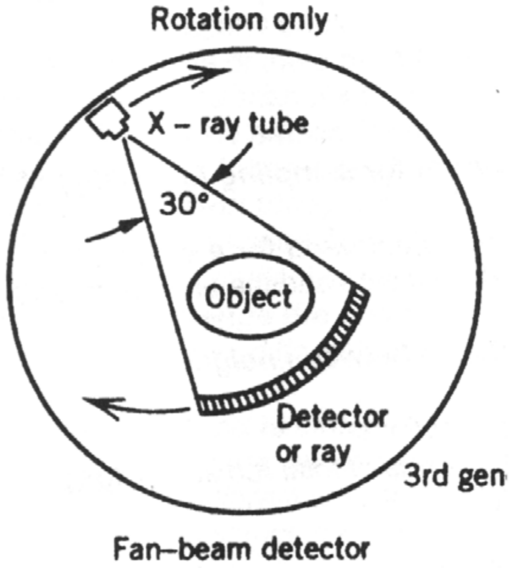

- Wide fan beam ($30^\circ \sim 60^\circ$) covering complete field of view
- 100s of detectors
- Only rotation, no translation
- Pulsed or continuous acquisition
- Fast (5 s / section)

Scanner geometry — generation 4

1977

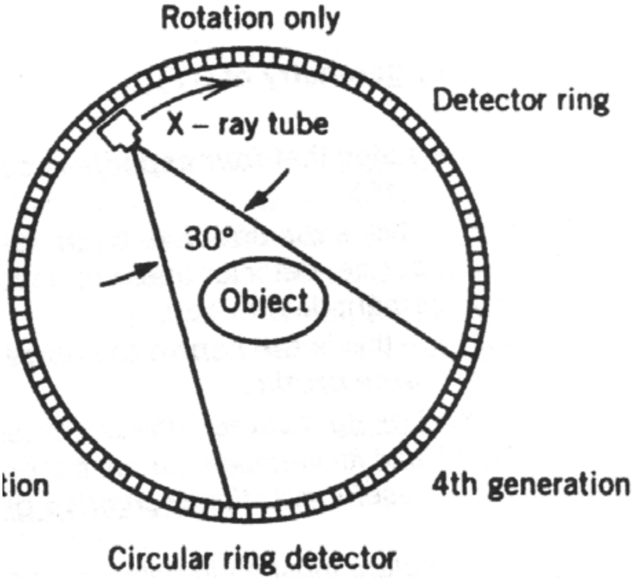

- Rotating source, stationary detector rings
- More expensive
- Avoids rotating contacts
- Fast

Scanner geometry — generation 5

Electron beam CT (EBCT, 1983)

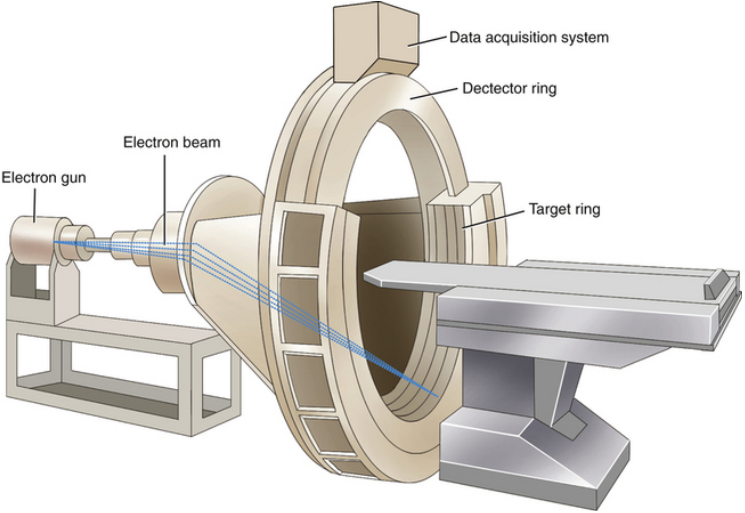

- No moving parts
- Directional X-ray source
- Extremely fast (beating heart)
- Lower signal to noise ratio and spatial resolution

CT X-ray sources

Similar but bigger than radiography X-ray sources

Typical properties of an X-ray tube used for CT compared to those of a conventional radiographic tube.

	Conventional X-Ray Tube	CT X-Ray Tube
Typical exposure parameters	70 kV, 40 mAs	120 kV, 10,000 mAs
Energy requirements	2,800 J	1,200,000 J
Anode diameter	100 mm	160 mm
Anode heat storage capacity	450,000 J	3,200,000 J
Maximum anode heat dissipation	120,000 J/min	540,000 J/min
Maximum continuous power rating	450 W	4000 W
Cooling method	Fan	Circulating oil

- Challenges: Power leads, cooling, vibration, ...

CT X-ray sources

Similar but bigger than radiography X-ray sources

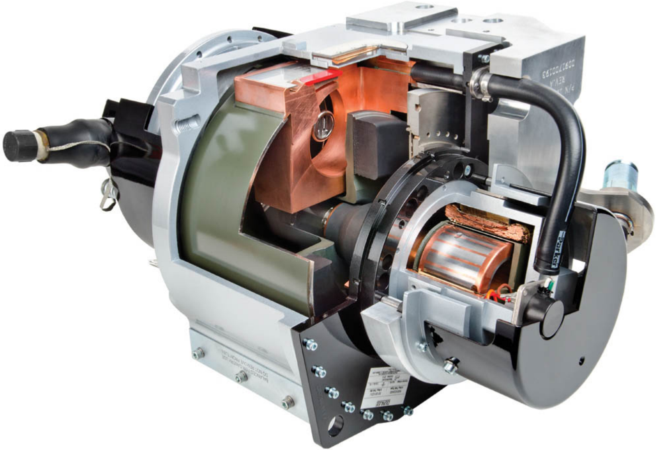

- Challenges: Power leads, cooling, vibration, . . .

CT X-ray sources - novel approach

Liquid anode tube: overcoming power density limitations of solid target X-ray tubes

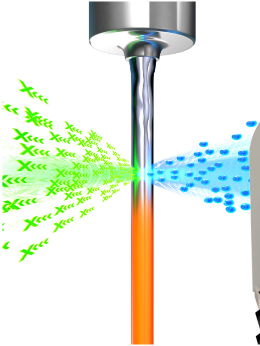

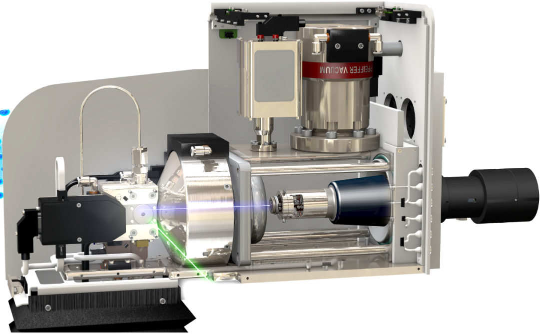

Liquid metal-jet tube:

- Heat dissipation problem nearly obsolete
- Small focal sizes viable (10-15µm) at high power ($\sim 500\,\mathrm{W}$)
  $\Rightarrow$ Allows for high magnification / system resolution

Filtering and collimation (1)

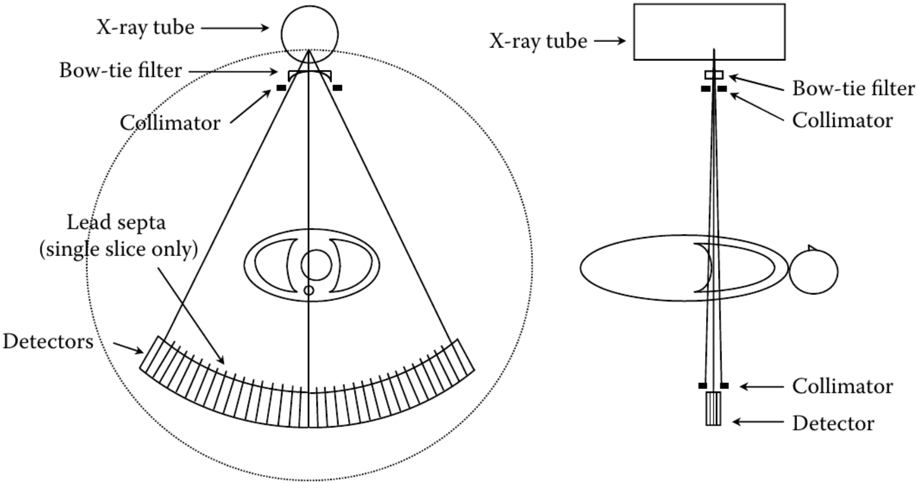

Filtering and collimation (2)

- Beam shaping (attenuate lateral part of the beam)

- Pre-patient and detector collimation — beam(slice) width

CT detector types

- Xenon ionization chamber detectors
  - Faster but less sensitive
- Scintillation detectors
  - More sensitive but slower (afterglow, scintillator dependent)

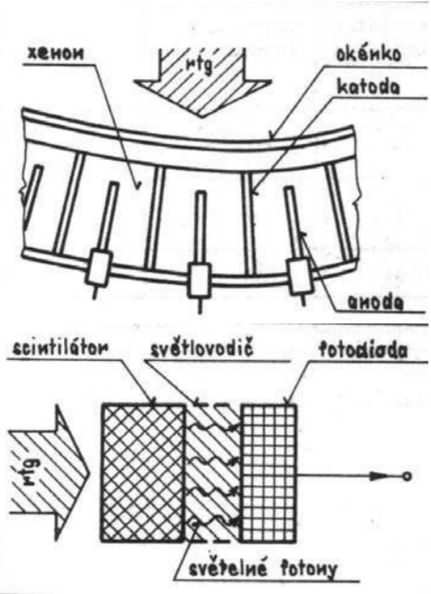

CT detector types

Properties of detectors in common use in CT scanning.

	Xenon Detectors	**Crystal Scintillator**	**Ceramic Scintillator**
Detector	High pressure (8–25 atm) Xe ionisation chamber	$CaWO_4$ + silicon photodiode	Gd_2O_2S + silicon photodiode
Detector array	Single chamber, divided into elements by septa	Discrete detectors	Discrete detectors
Signal	Proportional to ionisation intensity	Proportional to light intensity	Proportional to light intensity
Detector efficiency	40%–70%	95%–100%	90%–100%
Geometric efficiency (in fan direction)	>90%	>80%	>80%
Afterglow limitations	No	Yes	No
Detector matching	No	Yes	Yes

Scintillation detector construction

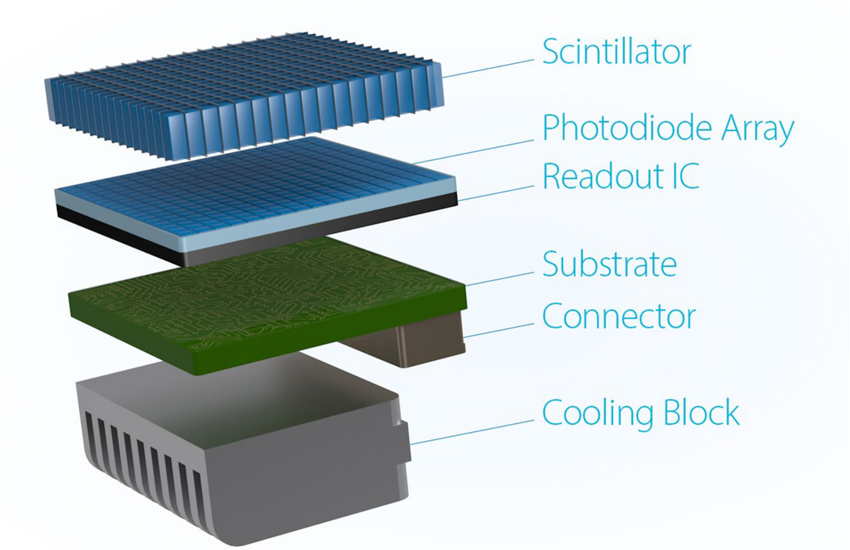

Scintillation detector construction

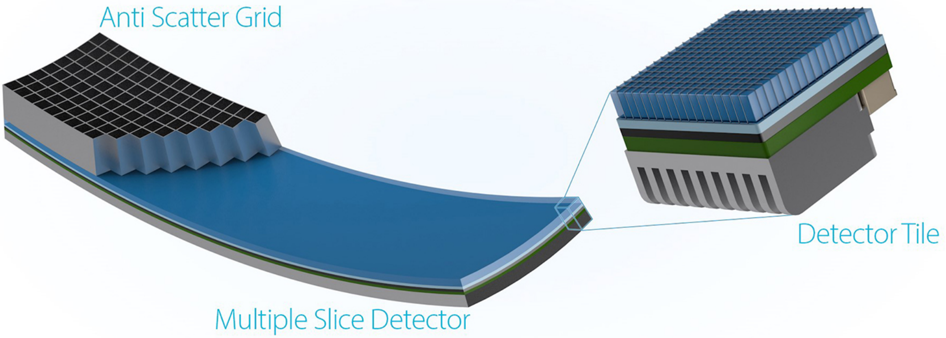

Multiple (e.g. 32, 64) slices $\longrightarrow$ acceleration

Scintillation detector construction

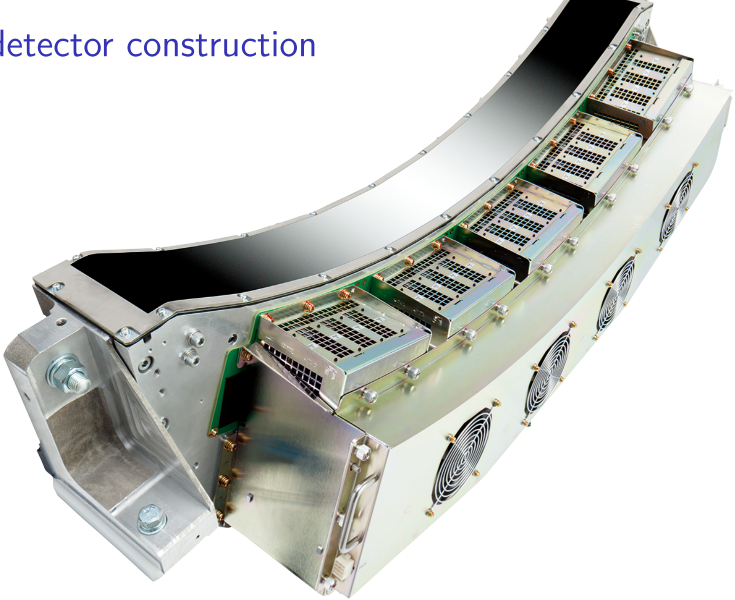

Multiple (e.g. 32, 64) slices $\longrightarrow$ acceleration

X-ray detectors: Photon counting detectors

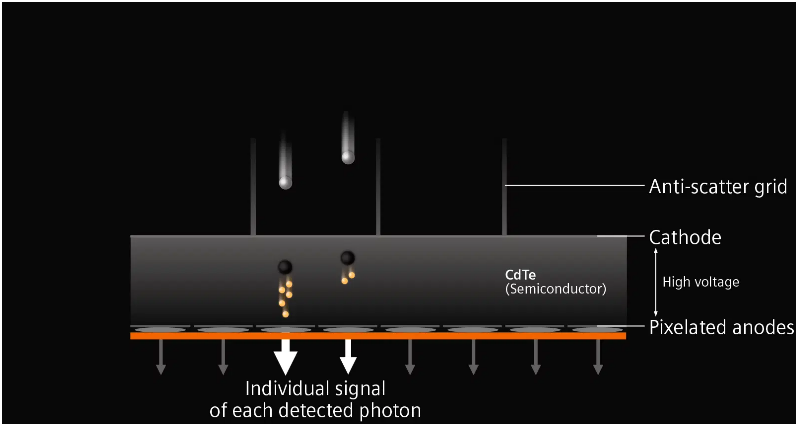

- Unlimited dynamic range and exposure time
- Detected count obeys Poisson distribution

Electric processing — corrections

- Offset correction (zero signal at rest)
- Normalization correction (x-ray source intensity fluctuation)
- Sensitivity correction (inhomogeneous detectors and amplifiers)
- Geometric correction
- Beam hardening correction
- Cosine correction (for fan beam geometry)

Introduction to CT

Hardware

Mathematics and Physics of CT

Radon transform

Attenuation along a line

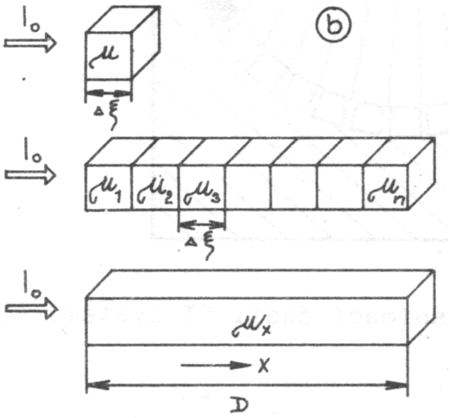

Homogeneous material (Beer-Lambert's law)

$$I = I_0 \mathrm{e}^{-\mu \Delta \xi}$$

Piecewise homogeneous material

$$I = I_0 \prod_{i=1}^{n} \mathrm{e}^{-\mu \Delta \xi} = I_0 \mathrm{e}^{-\Delta \xi \sum_{i=1}^{n} \mu_i}$$

Continuously varying $\mu(x)$, $x = i\Delta\xi$

$$I = I_0 \mathrm{e}^{-\lim_{\Delta\xi \to 0} \Delta\xi \sum_{i=1}^{n} \mu_i}$$
$$= I_0 \mathrm{e}^{-\int_0^D \mu(x) \mathrm{d}x}$$

Line integral for line L

$$= I_0 \mathrm{e}^{-\int_L \mu(\mathbf{x}) \mathrm{d}\mathbf{x}}$$

Hounsfield units

HU, CT number

$$CT = 1000 \frac{\mu - \mu_{\text{water}}}{\mu_{\text{water}}}$$

- Values between -1000 (air) and approximately 1000 (bones)
- Densities in HU are *reproducible* between devices
- To differentiate soft tissue types, tumor types etc.
- Accurate calibration is needed

Hounsfield units

HU, CT number

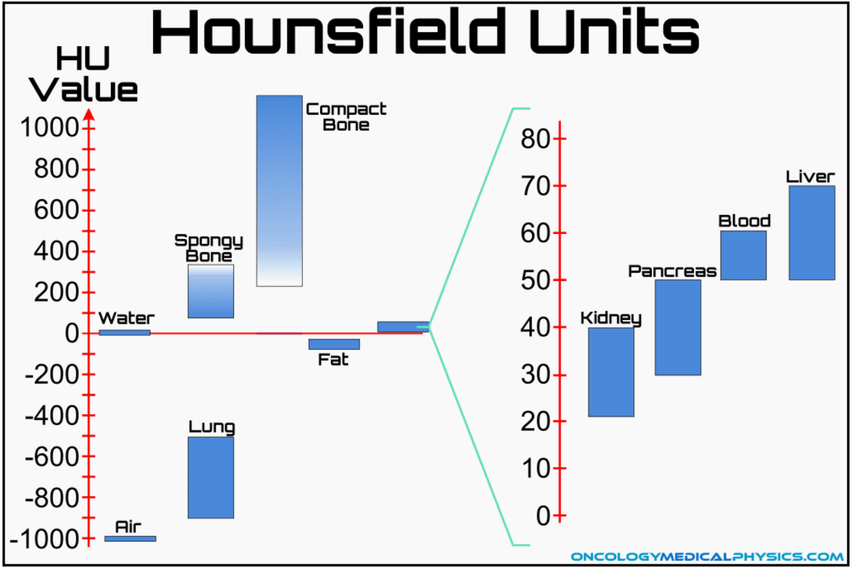

Beam hardening

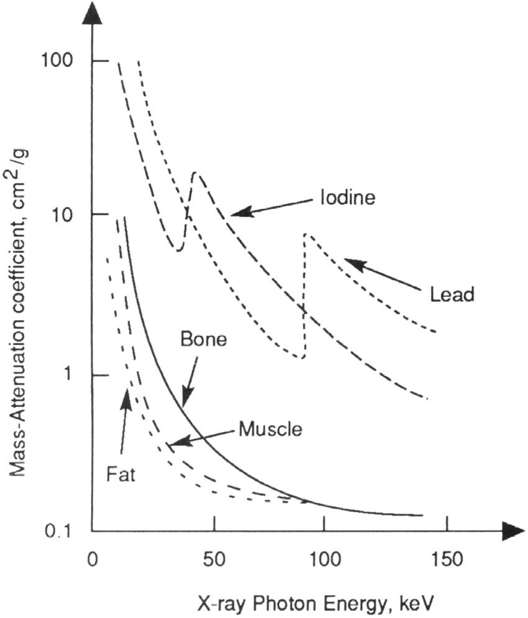

- Attenuation decreases with E

Beam hardening

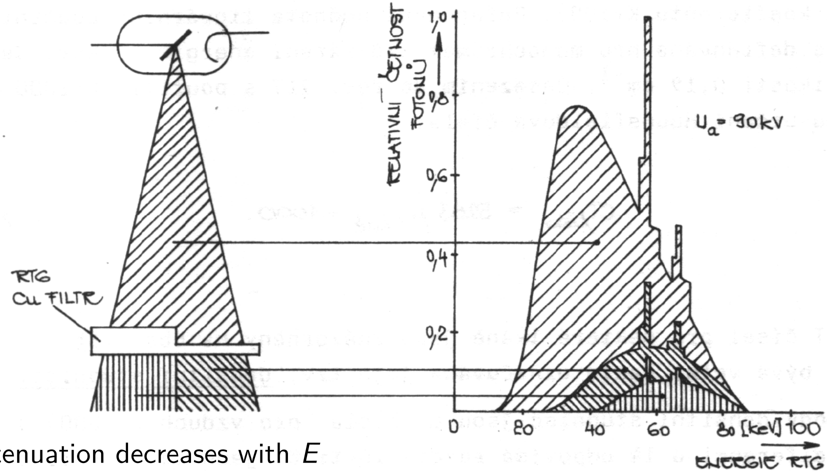

- Attenuation decreases with E
- $\longrightarrow$ low E rays are attenuated more
- $\longrightarrow$ mean E increases

Beam hardening

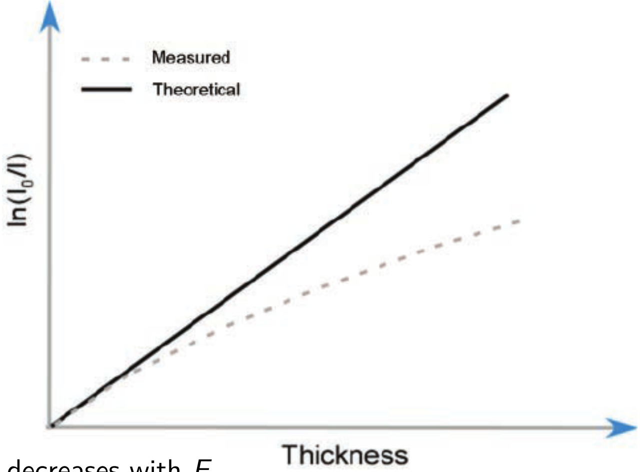

- Attenuation decreases with E
- $\longrightarrow$ low E rays are attenuated more
- $\longrightarrow$ mean E increases
- Measured attenuation $p = \log(I_0/I) <$ theoretically linear $\mu\Delta\xi$.

Beam hardening

- Attenuation decreases with E
- $\longrightarrow$ low E rays are attenuated more
- $\longrightarrow$ mean E increases
- Measured attenuation $p = \log(I_0/I) < $ theoretically linear $\mu\Delta\xi$.
- Beam hardening correction

Attenuation, interaction of radiation with matter

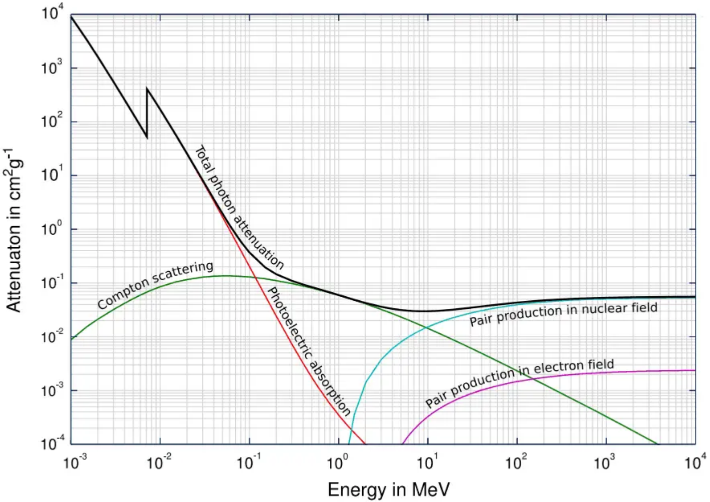

- "absorption edges" correspond binding energies of electrons from atom's shells.

Attenuation, materials

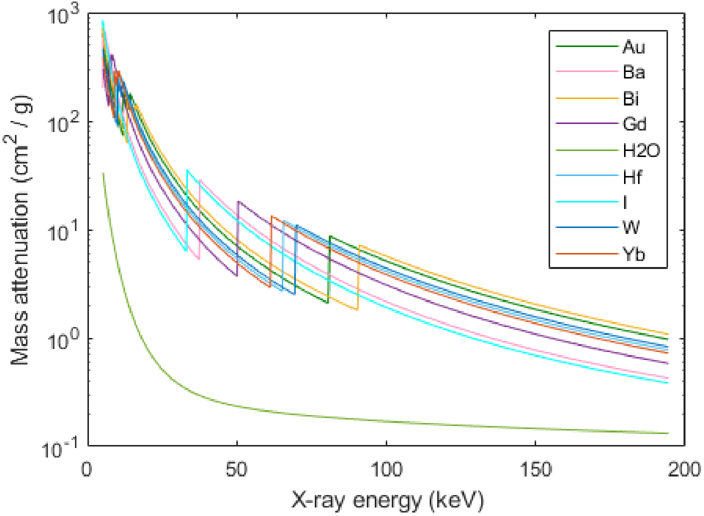

- high-Z candidate materials have been identified in recent years
- Extensive pre-clinical testing and method development required

Linear forward problem

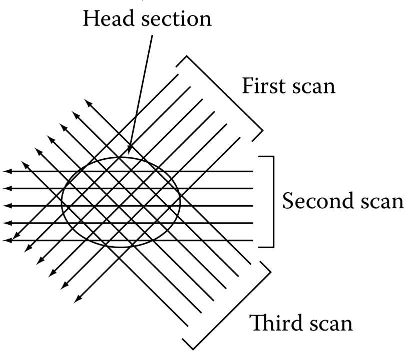

For N straight lines L_j, measure the attenuation

$$p_j = \log \frac{I_0^j}{I^j} = \int_{L_j} \mu(\mathbf{x}) \mathrm{d}\mathbf{x}$$

Assumptions

- Infinitely thin rays
- Straight lines — no scattering, reflection or refraction
- Monochromatic radiation — no beam hardening

(Assumptions can be relaxed but more complicated dependency.)

Linear forward problem

For N straight lines L_j, measure the attenuation

$$p_j = \log \frac{I_0^j}{I^j} = \int_{L_j} \mu(\mathbf{x}) \mathrm{d}\mathbf{x}$$

Assumptions

- Infinitely thin rays
- Straight lines — no scattering, reflection or refraction
- Monochromatic radiation — no beam hardening

(Assumptions can be relaxed but more complicated dependency.)

Discretization

$$\mu(\mathbf{x}) = \sum_{i=1}^{M} c_i \psi_i(\mathbf{x})$$

$\longrightarrow$ linear system of equations $\mathbf{L}\mathbf{c} = \mathbf{p}$

Integration lines in polar coordinates

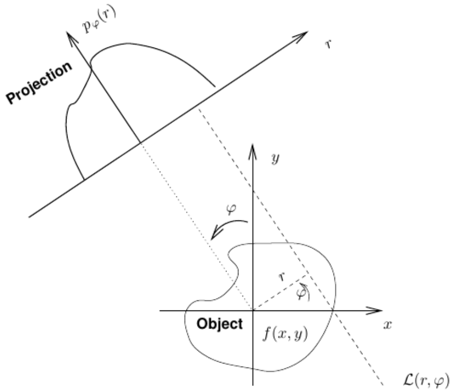

Describe integration lines by angle φ and offset r:

$$\begin{aligned} L(\varphi, r) &= \{(x, y) \in \mathbb{R}^2;\ x \cos\varphi + y \sin\varphi = r\} \\ &= \{(r\cos\varphi - t\sin\varphi, r\sin\varphi + t\cos\varphi);\ t \in \mathbb{R}\} \end{aligned}$$

Integration lines in polar coordinates

Describe integration lines by angle φ and offset r:

$$\begin{aligned} L(\varphi, r) &= \left\{(x, y) \in \mathbb{R}^2;\ x\cos\varphi + y\sin\varphi = r\right\} \\ &= \left\{(r\cos\varphi - t\sin\varphi, r\sin\varphi + t\cos\varphi);\ t \in \mathbb{R}\right\} \end{aligned}$$

Implicit line equation, $\mathbf{x} = (x, y)$

$$\left[\cos\varphi,\ \sin\varphi\right]\mathbf{x} = 0$$

Parametric line equation

$$\underbrace{\begin{bmatrix} \cos\varphi & -\sin\varphi \\ \sin\varphi & \cos\varphi \end{bmatrix}}_{\text{rotation matrix } R(\varphi)} \begin{bmatrix} r \\ t \end{bmatrix} = \mathbf{x}$$

Rotating system of coordinates

$$\begin{bmatrix} \xi \\ \eta \end{bmatrix} = R(\varphi) \begin{bmatrix} \xi' \\ \eta' \end{bmatrix}$$

$$\begin{bmatrix} \xi' \\ \eta' \end{bmatrix} = R^T(\varphi) \begin{bmatrix} \xi \\ \eta \end{bmatrix}$$

$$R^T(\varphi) = R(-\varphi)$$

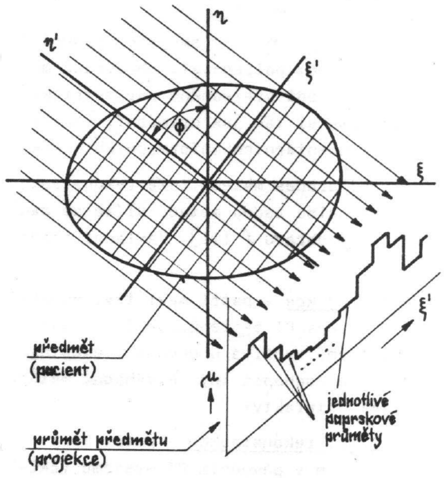

Projection

$$P_\varphi(\xi') = \int_{L(\varphi,\eta')} \mu(\mathbf{x}) \mathrm{d}\mathbf{x} = \int o(\xi, \eta') \mathrm{d}\eta'$$

Measurements

$$P_\varphi(\xi') = \log \frac{I_0}{I(\varphi, \xi')}$$

Change of variables

$$\xi' = r, \quad \eta' = t, \quad x = \xi, \quad y = \eta$$

Radon transform

Projection in polar coordinates:

$$P_\varphi(\xi') = \mathscr{R}\left[o(\xi,\eta)\right]$$
$$P_\varphi(\xi') = \int_L o(\xi,\eta)\mathrm{d}l$$

along the line L defined by φ a ξ':

$$\xi' = \xi\cos\varphi + \eta\sin\varphi$$

Equivalently

$$P_\varphi(\xi') = \int o(\xi'\cos\varphi - \eta'\sin\varphi, \xi'\sin\varphi + \eta'\cos\varphi)\mathrm{d}\eta'$$

Radon transform properties

Motivation: If a function f represents an unknown density, then the Radon transform represents the projection data obtained as the output of a tomographic scan. Hence the inverse of the Radon transform can be used to reconstruct the original density from the projection data, and thus it forms the mathematical background for tomographic reconstruction.

- **Linearity:**
$$\mathscr{R}[\alpha f + \beta g] = \alpha \mathscr{R}[f] + \beta \mathscr{R}[f]$$
- **Periodicity:**
$$P_{\varphi}(\xi') = P_{\varphi \pm 2\pi}(\xi') = P_{\varphi \pm \pi}(-\xi')$$

. . . and many others

Radon transform of a point

$$o(\xi,\eta) = \delta(\xi-\xi_0,\eta-\eta_0)$$
$$P_\varphi(\xi') = \mathscr{R}\big[o(\xi,\eta)\big] = \delta\big(\xi_0\cos\varphi+\eta_0\sin\varphi-\xi'\big)$$

...is a sinusoid with amplitude $\sqrt{\xi_0^2+\eta_0^2}$ and phase $\angle(\xi_0,\eta_0)$.

$$\xi' = \xi_0\cos\varphi+\eta_0\sin\varphi$$

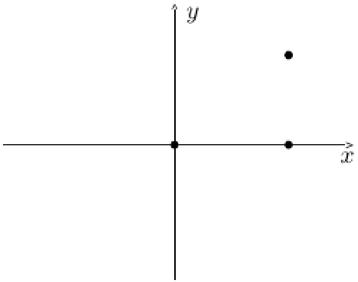

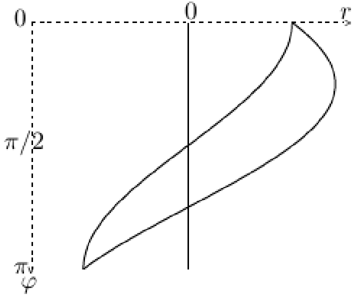

Radon transform

(sinogram)

of a disc

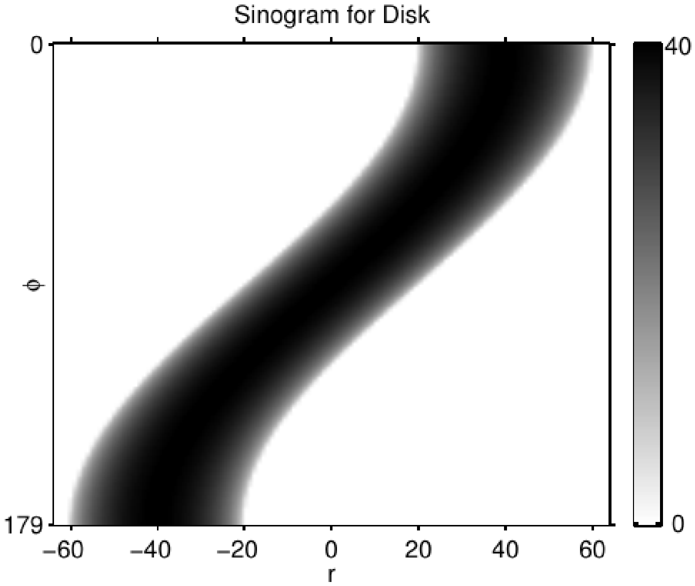

Radon transform

(sinogram)

of a square
(inverted)

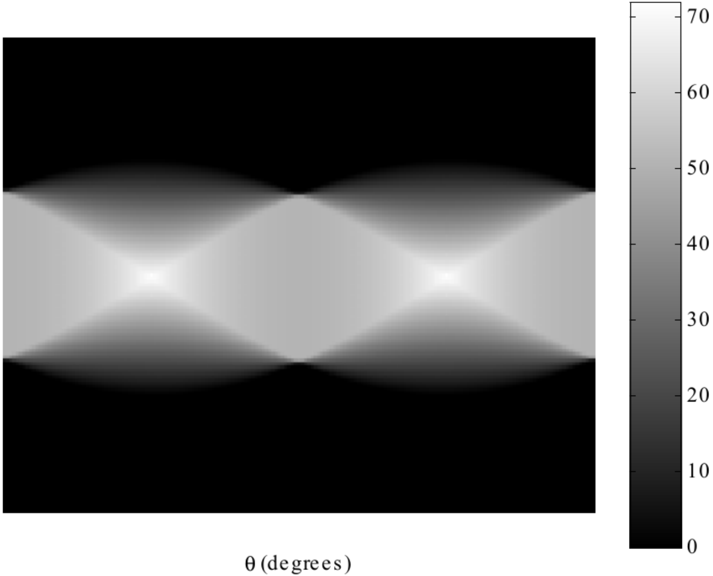

Radon transform
(sinogram)

of an object with
inserts (inverted)